Development of indium and cerium catalysts for the valorization of gaseous pollutants

Marta Coelho Silva (ist190525)
Instituto superior técnico

Abstract

Catalysts based on indium and cerium were synthesized using two different methods: the epoxide addition method and electrospinning technique aiming the study of the morphology effect (nanoparticles and fibers) and the In/Ce ratio on their catalytic performance. Supported Ni catalysts were also prepared by the incipient wetness impregnation method using pure metal oxides (In_2O_3, CeO_2) or InCe bimetallic oxides prepared by the epoxide addition method as supports. All catalysts were characterized by XRD, SEM/EDS, BET, H_2-TPR and oxidative dehydrogenation/dehydration of isopropanol to study its acid-base properties. The catalysts were studied in three main reactions aiming the valorization of pollutant gases, e.g., CO_2, N_2O, CH_4 and production of value-added hydrocarbons, namely: C_2 hydrocarbons via the oxidative coupling of methane and in particular ethylene via the oxidative dehydrogenation of ethane. The results obtained show that the catalysts are mainly catalytic active to produce ethylene via dehydrogenation of ethane using N_2O as oxidant, compared to those obtained using CO_2 and O_2 as oxidants, which was never reported in the literature. The best results were those obtained over the catalysts prepared by the incipient wetness impregnation method, 25% Ni/InCe(1:1) and 25% Ni/In_2O_3 that presents yields in ethylene almost the triple of those recorded over one of the most promising catalysts reported in the literature (25% Ni/InCe(1:1); C_2H_6 conversion =31%, C_2H_4 selectivity =42% versus VO_x/MCM-41, C_2H_6 conversion=8.5%, C_2H_4 selectivity =60%).

1. Introduction

Global industrialization, population growth and the need to produce more and more energy have raised the levels of carbon dioxide in the atmosphere to worrying levels, with its concentration reaching an unprecedented level in 2019 (≈ 411 ppm) and continuing with a growing trend.[1] The emitted CO_2 comes especially from the use of fossil fuels, the main contribution to global warming. Thereby, it is urgent to mitigate these emissions, to reduce their atmospheric concentration, fulfilling, for example, the objectives of the Paris Agreement. [2] Countries must strengthen decarbonization and mitigation measures for the effects of climate change, some of these measures are the capture and recovery of greenhouse gases, namely CO_2, CH_4 and N_2O. Therefore, catalytic reactions such as hydrogenation or electrochemical reduction of CO_2 are recognized as ways to solve problems related to this, as they will not only contribute to the reduction of CO_2 emissions, but also convert CO_2 into chemical products with high commercial value. e.g. methanol (CH_3OH) and other longer chain hydrocarbons (paraffins, olefins) [3]. Thus, the development of efficient catalysts for these reactions is a central and appealing theme.

The hydrogenation of CO_2 is a very challenging reaction since the CO_2 molecule is extremely stable. Carbon dioxide is a linear triatomic molecule, composed by one carbon atom covalently bonded to two oxygen atoms. The bond length between C (carbon) and O (oxygen) in molecular CO_2 is 1.17 Å [4] and its dissociation energy is 803 kJ/mol [5]. The combination of high symmetry, low polarity and high binding energy explains the chemically inert nature of CO_2, this characteristic makes its activation energetically demanding. Considering the

data available in the literature, the activity of the studied metals for CO_2 hydrogenation and methane production can be ordered as follows: Ru > Rh > Ni > Fe > Co > Os > Pt > Ir > Mo > Pd, thus the most active catalysts involve noble metals. Highlighting Ni as an excellent alternative [6].

The presence of ethane in the atmosphere is not significant, but its levels have also been increasing. [7] The oxidative dehydrogenation of ethane to produce ethylene is a very important reaction, as ethylene is widely used in the polymer industry, namely in the production of polyethylene. Ethylene is also used to produce various chemical compounds such as acetaldehydes, linear alcohols or vinyl acetates, fibers, rubbers and other materials that are widely used today.[8] Therefore, the growing need for light olefins (C_2) and the changing nature of the raw material has stimulated research to develop new routes for the process but steam cracking remains the most relevant route from an industrial point of view, responsible for around 97% of the total volume of ethane produced in the world.[9] However, the oxidative dehydrogenation of ethane ($C_2H_6 + \frac{1}{2}O_2 \rightarrow C_2H_4 + H_2O$, $\Delta H^0_{298} = -105\ kJ/mol$) is a more sustainable alternative that enables the production of ethylene at lower temperatures. Besides O_2, other oxidants have been explored for the dehydrogenation of ethane such as CO_2 and N_2O ($C_2H_6 + CO_2 \rightarrow C_2\ \ H_4 + H_2O + CO$, $\Delta H^0_{298} = -134\ kJ/mol$ and $C_2H_6 + N_2O \rightarrow C_2H_4 + H_2O + N_2$, $\Delta H^0_{298} = -187\ kJ/mol$, respectively) but the results remain at a level not adequate for an industrial application. The most studied catalysts for the dehydrogenation of ethane were vanadium and molybdenum oxides [10], due to their redox properties and their efficient performance in the oxidation of other alkanes, such as butane. Regarding the supports, the most studied has been aluminum oxide, as it allows better dispersion and facilitates the reduction of active sites increasing the reaction activity and selectivity [11]. The best results were obtained with V_2O_5/Al_2O_3, at 550 °C using CO_2 as oxidant, with 60% ethylene selectivity and 28% ethane conversion.[11] In addition to these catalysts, other transition metals were further studied, such as Ni, Mo, Cr, Fe, Co, as they have an excellent ability to adsorb and activate alkanes.[12] For example the catalyst Cr/Al_2O_3, at 700°C, using N_2O as oxidant, converted 43 % of the ethane to an ethylene selectivity of 51%.[13]

Herein, we report the synthesis of indium and cerium-based catalysts using two different methods: the epoxide addition method and electrospinning technique aiming the study of the morphology (nanoparticles and fibers) effect. Supported Ni catalysts were also prepared by the incipient wetness impregnation method using pure metal oxides (In_2O_3, CeO_2) or InCe bimetallic oxides prepared by the epoxide addition method as supports. All catalysts were characterized by XRD, SEM/EDS, BET, H_2-TPR and oxidative dehydrogenation/dehydration of isopropanol aiming the study of its acid-base properties. The study of their catalytic behavior was also undertaken aiming the valorization of pollutant gases, e.g., CO_2, N_2O, CH_4 and production of value-added hydrocarbons, in particular ethylene via the oxidative dehydrogenation of ethane using N_2O as oxidant.

1.1 Experimental

1.1.1. Catalyst preparation

Bimetallic oxide catalysts containing indium and cerium were prepared by two different methodologies: the electrospinning technique (as fibers) and the epoxide addition method (as aerogels). The obtained aerogels were also used as supports to prepare nickel catalysts by the incipient wetness impregnation method.

For the catalysts preparation by the electrospinning technique, 13.2552 g of PVP were dissolved in 40 mL of absolute ethanol (42wt.% PVP/absolute ethanol) and after total dissolution, the appropriate amounts of

indium nitrate (Thermo Scientific, 99.99%) and cerium nitrate hexahydrate (Aldrich, 99,999%) were added in order to obtain catalysts with the following molar ratios: InCe(3:1), 0.7652 g of $In(NO_3)_3.xH_2O$ and 0.3474 g of $Ce(NO_3)_3.6H_2O$; InCe(1:1), 0.4251 g of $In(NO_3)_3.xH_2O$ and 0.5789 g of $Ce(NO_3)_3.6H_2O$ and InCe(1:3), 0.2126 g of $In(NO_3)_3.xH_2O$ and 0.8684 g of $Ce(NO_3)_3.6H_2O$. These solutions were introduced into a 10 mL syringe with a stainless-steel needle with an internal diameter of approximately 1.2 mm and pumped at a rate of 1 mL/h after applying a voltage of 15 kV between the tip of the needle and the target, 10 cm apart. The collected fibers were subsequently calcined at 800 °C for 2 hours, with a temperature increase of 1 °C.min^{-1}.

The catalysts preparation by the epoxide addition method, starts by dissolving the metal salts, cerium chloride heptahydrate (Aldrich, 99.9%) and indium nitrate monohydrate (Thermo Scientific, 99.99%), in the respective proportions (as already mentioned in the electrospinning technique) in absolute ethanol until the complete dissolution of the salts, followed by the addition of propylene oxide (PO; Acros Organics, 99.5%), 3.8 mL, drop by drop with stirring. Then, the solution is allowed to stand at room temperature until complete gelation, which occurs in a few minutes. For example, in the case of the InCe(1:1) bimetallic oxide, 1.1177 g (3mmol) of $CeCl_3.7H_2O$ and 0.9565 g (3 mmol) of $In(NO_3)_3.1H_2O$ were dissolved in 6.3 ml of absolute ethanol and subsequently added 3.8 ml (55 mmol) of propylene oxide. The gel obtained was aged in absolute ethanol for 48 h at 50 °C and dried by the organic solvent sublimation method (OSSD), successively using solutions of 50, 80 and 100% acetonitrile/ethanol (v/v), each for 24 h at 50 °C and 24 h of drying at the same temperature. Finally, the aerogel obtained was calcined at 800 °C for 2 h, with a heating rate of 1 °C.min^{-1}. The solid obtained was subsequently sieved at 200 mesh (75 µm).

To prepare catalysts by the incipient wetness impregnation method, e.g., 25wt.% nickel supported catalysts, 165.2 mg of nickel nitrate hexahydrate (Scharlau, extra pure) dissolved in distilled water was added to 100 mg of support under vigorous stirring. Then, the mixture was taken to dryness in a sand bath at 60 °C under constant agitation, subsequently calcined at 500 °C for 2 hours, with a temperature increment of 1 °C.min^{-1} and sieved at 200 mesh (75 µm).

1.1.2. Catalyst characterization

The catalyst's crystalline structure was characterized by X-ray diffraction (powder) using a Bruker D2Phaser diffractometer (Cu, monochromatic radiation kα, λ=1.5406 Å). The operational settings were voltage=30 kV; current = 10 mA; 2θ over a range of 20–80° using a 0.03° step with 3.5 s per step. SEM-EDS measurements were performed at the Microlab of Instituto Superior Técnico using a ThermoScientific benchtop, Phenom ProX G6 model, with CsB6 filament scanning electron microscope aiming samples morphology studies and determination of their surface chemical composition.

To study their reducibility, Temperature programmed reduction analysis (H_2-TPR) was carried out using the ChemiSorb 2720 -ChemiSoft TPx device from Micromeritics with a 10% mixture of H_2 in argon, total flow of 20 mL/min, at a heating rate of 10 °C/min from room temperature to 1050 °C. Based on prior calibration measurements with NiO powders (Aldrich, 99.99995% purity), the integration of the experimental H_2-TPR curves allow to assess quantitative H_2-uptakes.

The specific surface areas of the catalysts were measured using the Brunauer-Emmett-Teller method, involving the adsorption of nitrogen at the temperature of liquid nitrogen and determination of the surface area

through the consumption of nitrogen corresponding to the formation of the monolayer. For this purpose, the Micromeritics ChemSorb 2720 multifunctional device was used, using a mixture of 30% N_2 in He (Liquid Air, 99.9995%): P/P_0 = 0.3 and a total flow of 20 mL.min^{-1} and specific Pyrex reactors provided by the brand. All samples were submitted to to 3 cycles of N_2 adsorption (using liquid nitrogen, negative peaks) and desorption (when the liquid nitrogen is removed and the sample is allowed to return to room temperature, positive peaks).

Finally, to assess the acid-base properties of the catalysts, studies using a model reaction, the dehydrogenation/dehydration of 2-propanol (isopropanol) were undertaken. The tests were performed in a fixed-bed U-shaped Pyrex reactor at atmospheric pressure, in a temperature range between 175 to 275 °C. The reaction was conducted under a continuous flow of a mixture of 0.25% (v/v) of isopropanol in air N_2/O_2:80/20 (v/v) (Air Liquide, 99.9995% purity) with a Gas Hourly Space Velocity (GHSV) of 1012 mL/$g_{catalyst}$·h and a O_2 to isopropanol molar ratio of 10. Gas chromatography was used to analyse the composition of the reactor outlet gas. An Agilent 7280D chromatograph equipped with a flame ionization detector (FID) and a capillary column HP_PLOT_U, L = 25 m, ID = 0.32 mm was used for such purpose. From the ratio between the selectivity of acetone (vA) and propene (vP), a relative scale of basicity (vA/vP) was built.

1.1.3. Catalytic tests

All catalytic tests were performed continuously and at atmospheric pressure. The composition of the gas leaving the reactor was analyzed online by gas chromatography, using an Agilent 4890D chromatograph, equipped with a thermal conductivity detector (TCD) and a Restek ShinCarbon column (L = 2.0 m, Φ = 1/8 in, ID = 1 mm, 100/200 mesh), for the detection of reactants and products. Injection is performed using a 6-port valve with a 250 µL internal loop, pneumatically actuated. To avoid contamination of the column with water, the output stream is cooled in an ice-water bath in a trap.

A U-shaped quartz reactor was used, with an internal diameter of 9 mm and 1 mm of thickness, with an internal volume of approximately 7 cm^3. The reaction temperature was controlled by a thermocouple placed near the catalytic bed. In terms of ratio oxidant/C_2H_6=10 was used (after optimization), and the effect of GHSV was studied between 3500 and 15000 mL/g_{cat}.h and the later chose to prevent any diffusional problems, an optimized catalyst mass between 10-20 mg was used. To control each gas flows, mass flows controllers (Aalborg series A) were used. For the reactions with O_2 and N_2O, temperatures of 350 to 550 °C were used, whereas for the reaction with CO_2 the temperatures were from 500 to 700 °C. Conversions, selectivity's and yields were calculated from the following equations. All reported results represent catalytic activity values at steady state after 1 hour of reaction.

$$C_2H_6\ Conversion\ (\%) = \frac{[C_2H_6]_i - [C_2H_6]_f}{[C_2H_6]_i} \times 100, \qquad C_xH_y\ Selectivity\ (\%) = \frac{[C_xH_y]_f}{[C_2H_6]_i - [C_2H_6]_f} \times 100$$

$$C_xH_y\ Yield\ (\%) = \frac{C_2H_6\ Conversion\ (\%) \times C_xH_y\ Selectivity\ (\%)}{100}$$

2. Results and discussion

Figure 1 shows the X-ray diffractograms obtained for the indium-cerium bimetallic oxides prepared by the epoxide addition method (Figure 1a) and for the Ni supported catalysts (Figure 1b), after calcination at 800 °C. The diffractograms obtained for the fiber's catalysts were very similar to those of the aerogels, so they are not

presented. For the bimetallic oxides (Figure 1a), two cubic oxide phases were identified, In_2O_3 and CeO_2. For the supported Ni catalysts (Figure 1b) three cubic oxide phases could be identified, CeO_2, In_2O_3 and NiO.

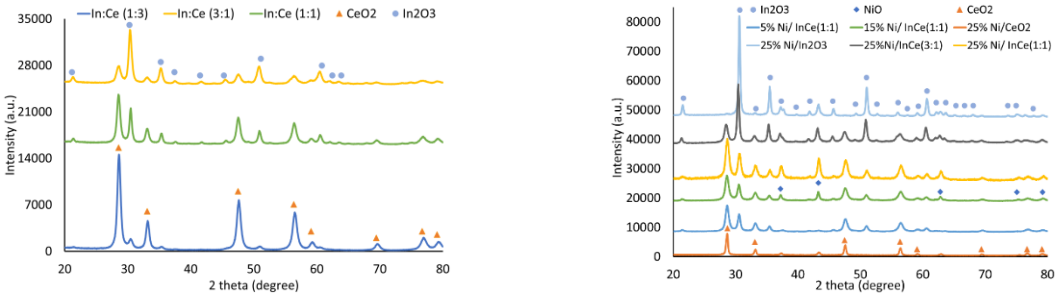

(a) (b)

Figure 1 - X-ray diffraction patterns obtained after calcination for the bimetallic oxides (a) and for the Ni supported catalysts (b).

Figure 2 shows the diffractograms obtained after H_2-TPR for the catalysts synthesized by the epoxide method and those obtained by the incipient wetness impregnation method (Figure 2a and b, respectively). Compared to Figure 1 diffractograms, the samples analyzed after H_2-TPR are more crystalline, which can be attributed to the high temperature reached during this study (> 1000 °C). The observed phases for the aerogels are metallic indium ascribed to the complete reduction of indium oxide ($In^{3+} \longrightarrow In^0$) and CeO_2, indicating that CeO_2 only reduces partially or that at the time of the XRD analysis, Ce_2O_3 (Ce^{3+}) may have already been oxidized to Ce^{4+}. For the compounds obtained by the incipient wetness impregnation method Figure 2b not only metallic indium and cerium oxide were detected but also metallic Ni from the complete reduction of NiO and some intermetallic phases InNi (In_3Ni_2, InNi and $InNi_2$). The formation of these intermetallic compounds is known from the literature [14] and depends on the amounts of In and Ni present in the samples: the trigonal phase In_3Ni_2 was identified in the samples 25% Ni/In_2O_3, 5% Ni/InCe(1:1), 15% Ni/InCe(1:1) and 25%Ni/InCe(3:1); the hexagonal phase $InNi_2$ (greater amount of Ni), was identified at 15% and 25%Ni/InCe(1:1), 25%Ni/InCe(3:1) and 25%Ni/InCe(1:3) and the InNi phase (same amount of In and Ni) was only identified in 25%Ni/InCe(3:1).

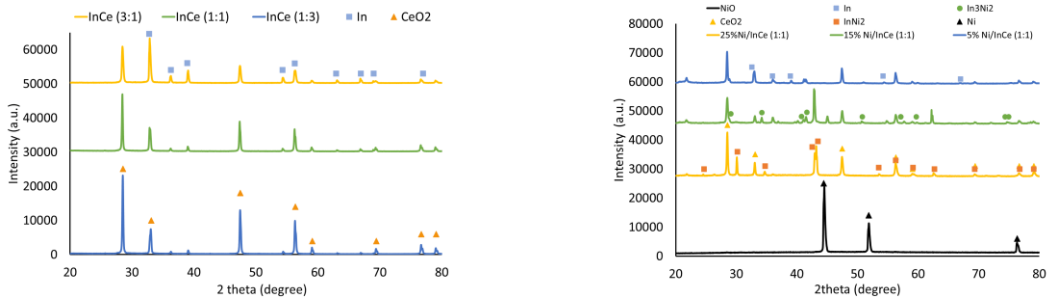

(a) (b)

Figure 2 - X-ray diffraction patterns obtained after H_2-TPR study for the bimetallic oxides (a) and for the Ni supported catalysts (b).

Figure 3 shows representative SEM images of the catalyst's morphology. The catalysts obtained by the electrospinning technique have a fiber morphology (Figure 3a) that in some points are more brittle, short, and thin, which is partly attributable to the high calcination temperature used to remove the PVP, which serves as a matrix for fiber structure. The fibers have diameters close to 1 µm. Through Figures 3b and 3c, it´s noticeable the clusters of nanoparticles of various sizes with a spongy aspect. The SEM images for the other ratios InCe are very similar to Figures 3b and 3c.

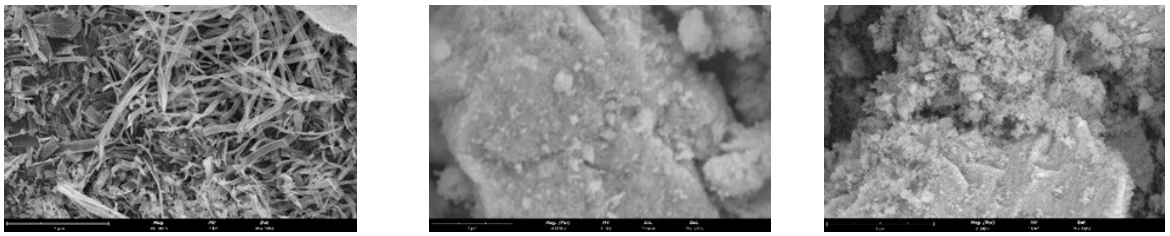

(a) (b) (c)

Figure 3 – SEM images of InCe (1:1) obtained from electrospinning (a), epoxide method (b) and dry impregnation with 25% of Ni (c), after calcination. Ampliation 10000 X.

The H_2-TPR profiles obtained are presented in Figure 4, for the bimetallic oxide aerogels (Figure 4a) and fibers (Figure 4b) and for the Ni supported catalysts (Figure 4c), the H_2-TPR profiles obtained for the fibers are very similar to the aerogels. Pure oxides are also shown and have only one peak, for the In_2O_3 at 650 °C, corresponding to the total reduction of In_2O_3 to metallic In, equation 1, and for CeO_2 at 784 °C, that may be attributable to the partial or total reduction of Ce^{4+} to Ce^{3+}. Although the Ce_2O_3 phase does not appear in XRD patterns, the quantification after H_2-TPR (Figure 2a), considering the equation 2, seems to confirm the partial/total reduction of the Ce^{4+} to Ce^{3+}. Regarding the bimetallic oxides, there are a more intense peak at higher temperatures (500-600°C) that reflects the reduction of indium (equations 3 to 5) and a less intense peak at the lower temperature (200-300 °C) that normally corresponds to the reduction of surface oxygen, but considered part of indium reduction process [15]. The less intense peak appears at temperatures above 700 °C and is attributed to the reduction of CeO_2 to Ce_2O_3 [16].

Figure 4c shows the H_2-TPR profiles obtained for different loadings of Ni supported on InCe (1:1) bimetallic oxides aerogels. The reduction profile is now composed by one part that contains that corresponding to the reduction of NiO (≈ 400 °C, blue area) and other that is linked to the reduction of In_2O_3 present in the InCe(1:1) bimetallic oxide (500-600 °C, yellow area). The CeO_2 still has no total reduction, but its profile is clearly seen at ≈700 °C. The profile part linked to the reduction of NiO is complex since the addition of nickel facilitates the reduction of indium oxide, moving its T_m to lower temperatures but this complexity is also related to the reduction of Ni and In and formation of intermetallic compounds InNi ($InNi_2$, InNi, In_3Ni_2) that increase with the amount of Ni [14].

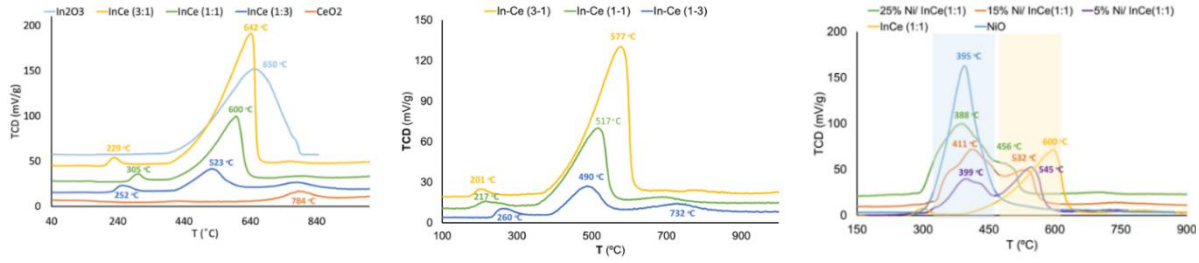

(a) (b) (c)

Figure 4 - H_2-TPR profiles obtained for catalysts synthesized by the epoxide addition method (a) and by the electrospinning method (b) and by the incipient wetness impregnation (c).

The experimental consumption of H_2 moles was calculated through the equations 1 to 5 and a good match was found between the experimental and theoretical consumption of H_2, which ratio varies between 0.9 and 1.1, regardless of the preparation method, except for the pure oxide CeO_2 (ratio obtained 0.5).

$$In_2O_3 + 3H_2 \rightarrow 2In + 3H_2O \quad (1)$$

$$2CeO_2 + H_2 \rightarrow Ce_2O_3 + H_2O \quad (2)$$

$$In_2O_3.2CeO_2 + 3H_2 \rightarrow 2In.2CeO_2 + 3H_2O \quad (3)$$
$$3In_2O_3.2CeO_2 + 9H_2 \rightarrow 6In.2CeO_2 + 9H_2O \quad (4)$$
$$In_2O_3.6CeO_2 + 3H_2 \rightarrow 2In.6CeO_2 + 3H_2O \quad (5)$$

The study of catalysts acid-base properties was accomplished using the dehydration/dehydrogenation reaction of isopropanol as a model reaction. The results are presented in Figure 5. The least basic catalysts are pure oxides (indium and cerium) in aerogel form. In the case of the bimetallic oxides, the basicity increases with the amount of cerium and the most basic bimetallic oxides are those with the lowest InCe molar ratio (InCe ratio (1:3)) obtained either by the epoxide addition method or by electrospinning technique.

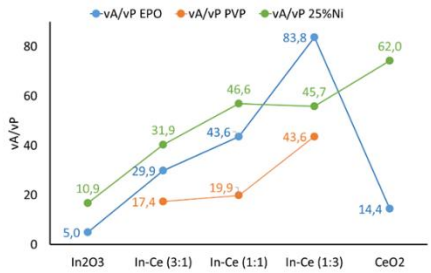

Figure 5 - Relative basicity of the InCe bimetallic oxides and respective pure oxides obtained by the epoxide addition method (blue line) and electrospinning (orange line) and impregnated with 25% Ni (green line), at T= 300 ˚C.

It is also possible to state that the fibers are less basic than the aerogels. In the case of the catalysts obtained by the impregnation method, there is again an increase in basicity with the increase in the cerium content in the support and, comparing the three preparation methods, the nickel catalysts obtained by impregnation are the most basic.

2.1. Catalytic tests

2.1.1. Oxidative Dehydrogenation of Ethane

The oxidative dehydrogenation of ethane was studied, and key experimental parameters optimized, namely: oxidant nature, molar ratio between oxidant and ethane and the pre-reduction of the catalysts (Figure 6). The results obtained show that the pretreatment enhances the production of ethylene (Figure 6a) and nitrous oxide is the most appropriate oxidant (Figure 6b), whereas a molar ratio of 10 ratio is the better commitment between ethane conversion and ethylene selectivity (Figure 6c). Indeed, the reaction was studied with an appropriate GHSV to avoid diffusional problems of mass or heat and it was possible to concluded that with N_2O, in the tested temperatures, the catalysts present has always higher ethylene yields than those obtained with the remaining oxidants (O_2, CO_2). CO_2 gives intermediate values, whereas the poor results were those obtained with O_2. For what concern the effect of the molar ratio between N_2O / ethane on catalytic activity, Figure 6c shows that there is an increase in the conversion of the ethane with the increase in the ratio, while ethylene selectivity decreases. However, it was concluded that the 10 ratio has a better commitment between ethane conversion and ethylene selectivity, since for higher ratios there is a significant decrease in ethylene selectivity. Thus, the ratio of 10 and N_2O with pretreated catalysts were chosen for the remaining catalytic tests.

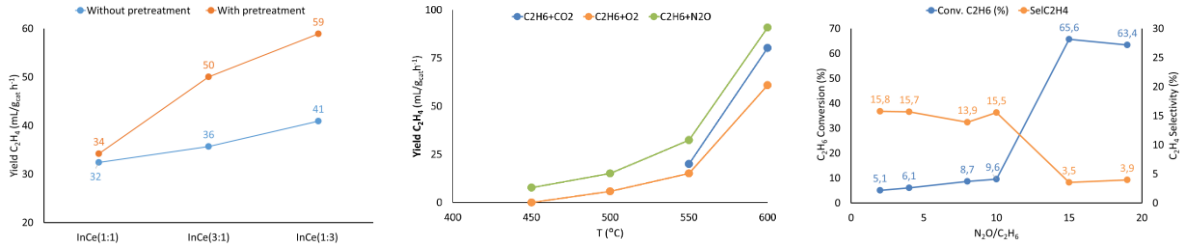

(a) (b) (c)

Figure 6 - Influence of the pretreatment (a) influence of the oxidant on ethylene yield (b) and influence of the ratio N_2O / ethane (c) for the aerogel InCe (1:1) catalyst. Reaction Conditions: N_2O / C_2H_6 = 10, GHSV = 7500 ml C_2H_6 / gcat.h), with reduction pretreatment.

After these preliminary optimization studies, the effect of the reaction temperature was also undertaken (Figure 7). As can be seen from Figure 7a, except for In_2O_3, all other prepared oxides have a positive influence on the reaction as they present higher conversions than those obtained during the blank test. It is also possible to observe that the reaction thermodynamics represented by the blank test (blank curve) has a great influence on the conversion of ethane only for temperatures ≥ 600°C. Thus, any comparison in the kinetic regime must be done using values obtained at lower temperatures, lower than 600°C, which was done.

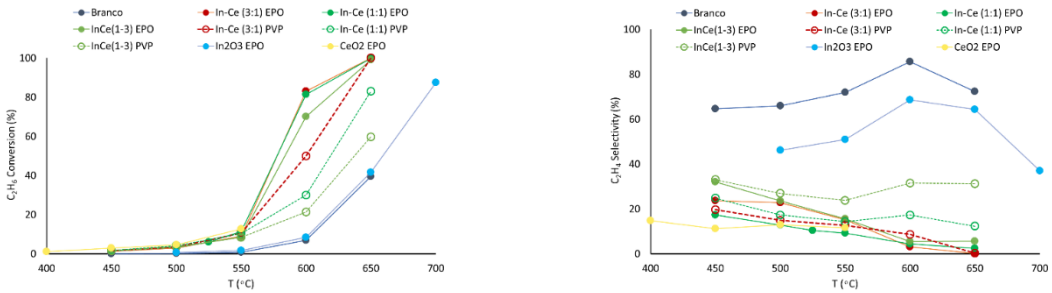

(a) (b)

Figure 7 – (a) C_2H_6 conversion (%), (b) selectivity of ethylene (%) as a function of temperature for catalysts in aerogel and fiber. N_2O / C_2H_6 = 10, GHSV = 7500 ml C_2H_6 / g_{cat}.h), with reduction pretreatment.

Figure 8 show the effect of the morphology on the catalysts' performance. It is possible to verify that, in general, using fibers higher ethylene yields can be archived that increase with the increase in the amount of cerium in the catalyst (Figure 8a). Which also happens over the aerogels. Figure 8b correlates the ethylene yield with CeO_2 crystallites sizes. For clarity reasons, the In_2O_3 crystallites sizes are not presented in the chart but follow the same trend. Therefore, it can be said that the yields in ethylene increases with the crystallites size, which is not so common since normally an inverse correlation can be found in the literature [17].

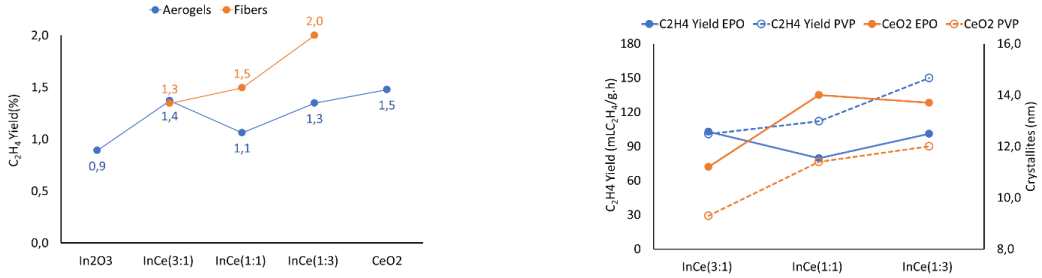

(a) (b)

Figure 8 - Catalytic Ethylene Yield results (a) and its correlation with the crystallites size (b), T=550°C, N_2O / C_2H_6 = 10, GHSV = 7500 ml C_2H_6 / g_{cat}.h), with pre-treatment reduction.

Figure 9 shows the effect of the catalyst's basicity (relative basicity, vA/vP) on the production of ethylene over aerogels and fibers. Regarding the aerogels (Figure 9a), the increasing tendency of the ethylene yield is in

accordance with the growing trend of basicity, except in the InCe (3:1). For the fibers (Figure 9b), the same effect is observed, the ethylene yield is enhanced by the catalysts' basicity.

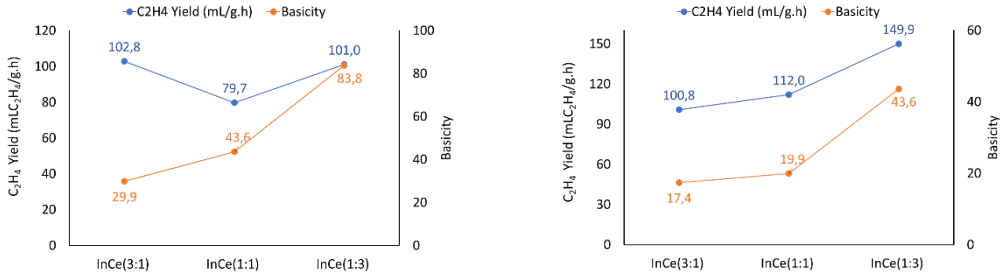

(a) (b)

Figure 9 – Correlation between ethylene yield and basicity to (a) aerogels and (b) fibers, T = 550° C, N_2O / C_2H_6 = 10, GHSV=7500 mL C_2H_6 / g_{cat}.h), with pretreatment.

Finally, Figure 10 presents the catalytic results for the supported Ni catalysts at 500°C. Again, the ethane conversion increases with the increase of content of cerium, except for the 25%Ni/In_2O_3, while ethylene selectivity has the opposite behavior (Figure 10a). Catalysts 25%Ni/In_2O_3 and 25%/InCe (1:1) exhibit very similar results that represent the most appropriate commitment between conversion and selectivity.

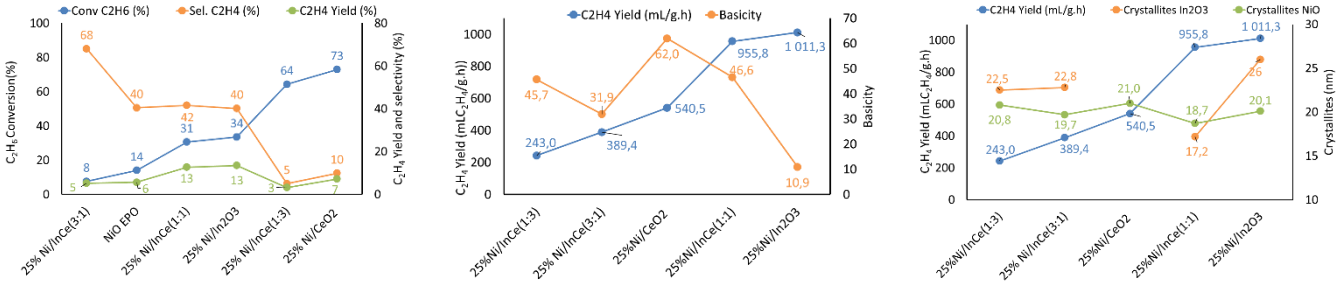

(a) (b) (c)

Figure 10 – Ethane conversion (%) and Ethylene yield (%) and selectivity (%) for the Ni supported catalysts (a). Correlation between ethylene performance and basicity (b) and crystallites (c) for the Ni supported catalysts, T= 500° C, N_2O/C_2H_6=10, GHSV=7500 mL C_2H_6 / g_{cat}.h), with pretreatment.

Regarding the effect of relative basicity (vA/vP) and the crystallites size (In_2O_3, NiO) on the activity of these catalysts, Figures 10b and 10c show the influence of both on ethylene performance. The obtained results do not show a specific trend with the increase of ethylene yield, in the case of the catalysts with bimetallic supports the more active is the more basic, 25% Ni/InCe(1:1), however the catalyst 25% Ni/In_2O_3 which has a slightly higher yield is the least basic. Whereas for what concerns the In_2O_3 crystallites size it follows the expected inverse direction of increased ethylene yield. Regarding the NiO (CeO_2 crystallites size are not presented in the figure, as they have very similar values), the values are very close, which unable any conclusion.

3. Conclusions

In the present work indium-cerium bimetallic oxide catalysts with different morphologies and Ni supported catalysts were prepared, characterized, and tested to produce ethylene via the oxidative dehydrogenation of ethane. The results obtained show that the best results were obtained with N_2O as oxidant, which was never reported in the literature. Moreover, the best results were those obtained over catalysts prepared by the incipient wetness impregnation method, 25% Ni/In_2O_3 and 25% Ni/InCe(1:1) that presents yields in ethylene almost the triple of those recorded over one of the most promising catalysts reported in the literature (25% Ni/InCe(1:1); C_2H_6 conversion =31%, C_2H_4 selectivity =42 versus VO_x/MCM-41, C_2H_6 conversion=8.5%, C_2H_4

selectivity =60%). The main factors that seem to contribute to catalysts' performance are the oxygen lability (catalysts reducibility) and their acid-base properties. The catalysts' reducibility is very similar for the aerogels and fibers morphologies: In_2O_3 reduces completely to metallic In and CeO_2 reduces only partially but maintains its structure. In the case of Ni supported catalysts, indium and nickel oxides reduce to the metallic forms with formation of intermetallic compounds (In_3Ni_2, InNi, $InNi_2$), which presence negatively influence their catalytic behavior. In general, the catalysts are basic, and their basicity strength influences positively their catalytic properties. Aerogels have a higher basicity than the fibers and Ni supported catalysts have the highest basicity and in general are the most active. In conclusion, indium - cerium-based bimetallic oxide catalysts and Ni supported catalysts on ceria and In_2O_3 could be a real alternative aiming the production of ethylene via oxidative dehydrogenation of ethane using nitrous oxide as oxidant.

4. References

[1] S. Dang *et al.*, «A review of research progress on heterogeneous catalysts for methanol synthesis from carbon dioxide hydrogenation», *Catal. Today*, vol. 330, pp. 61–75, jun. 2019, doi: 10.1016/j.cattod.2018.04.021.

[2] BP Statistical Review of World Energy, «Statistical Review of World Energy 2021», 70th edition, 2021.

[3] X.-Y. Meng, C. Peng, J. Jia, P. Liu, Y.-L. Men, e Y.-X. Pan, «Recent progress and understanding on In2O3-based composite catalysts for boosting CO2 hydrogenation», *J. CO2 Util.*, vol. 55, p. 101844, jan. 2022, doi: 10.1016/j.jcou.2021.101844.

[4] H. Tian, D. Maciążek, Z. Postawa, B. J. Garrison, e N. Winograd, «C-O Bond Dissociation and Induced Chemical Ionization Using High Energy $(CO_2)_n^+$ Gas Cluster Ion Beam», *J. Am. Soc. Mass Spectrom.*, vol. 30, n.º 3, pp. 476–481, mar. 2019, doi: 10.1007/s13361-018-2102-z.

[5] J. Wang *et al.*, «CO_2 Hydrogenation to Methanol over In_2O_3-Based Catalysts: From Mechanism to Catalyst Development», *ACS Catal.*, vol. 11, n.º 3, pp. 1406–1423, fev. 2021, doi: 10.1021/acscatal.0c03665.

[6] M. Younas, L. Loong Kong, M. J. K. Bashir, H. Nadeem, A. Shehzad, e S. Sethupathi, «Recent Advancements, Fundamental Challenges, and Opportunities in Catalytic Methanation of CO_2», *Energy Fuels*, vol. 30, n.º 11, pp. 8815–8831, nov. 2016, doi: 10.1021/acs.energyfuels.6b01723.

[7] J. Peischl *et al.*, «Quantifying Methane and Ethane Emissions to the Atmosphere From Central and Western U.S. Oil and Natural Gas Production Regions», *J. Geophys. Res. Atmospheres*, jul. 2018, doi: 10.1029/2018JD028622.

[8] S. Seifzadeh Haghighi, M. R. Rahimpour, S. Raeissi, e O. Dehghani, «Investigation of ethylene production in naphtha thermal cracking plant in presence of steam and carbon dioxide», *Chem. Eng. J.*, vol. 228, pp. 1158–1167, jul. 2013, doi: 10.1016/j.cej.2013.05.048.

[9] J. V. F. Moreira, «Steam Cracking: Kinetics and Feed Characterisation». IST, 2015. [Em linha]. Disponível em: Corpus ID: 109927221

[10] V. Cortés Corberán, «Nanostructured Oxide Catalysts for Oxidative Activation of Alkanes», *Top. Catal.*, vol. 52, n.º 8, pp. 962–969, jul. 2009, doi: 10.1007/s11244-009-9246-9.

[11] J. Le Bars, A. Auroux, M. Forissier, e J. C. Vedrine, «Active Sites of V2O5/γ-Al2O3Catalysts in the Oxidative Dehydrogenation of Ethane», *J. Catal.*, vol. 162, n.º 2, pp. 250–259, set. 1996, doi: 10.1006/jcat.1996.0282.

[12] C. Wang *et al.*, «Main-Group Catalysts with Atomically Dispersed In Sites for Highly Efficient Oxidative Dehydrogenation», *J. Am. Chem. Soc.*, p. jacs.2c04926, ago. 2022, doi: 10.1021/jacs.2c04926.

[13] Y. Zhang, Suresh Kumar Megarajan, X. Xu, J. Lu, e H. Jiang, «Catalytic Abatement of Nitrous Oxide Coupled with Ethane Oxydehydrogenation over Mesoporous Cr/Al2O3 Catalyst», *Catalysts*, vol. 7, n.º 5, p. 137, mai. 2017, doi: 10.3390/catal7050137.

[14] J. Guo, Z. Wang, J. Li, e Z. Wang, «In–Ni Intermetallic Compounds Derived from Layered Double Hydroxides as Efficient Catalysts toward the Reverse Water Gas Shift Reaction», *ACS Catal.*, vol. 12, n.º 7, pp. 4026–4036, abr. 2022, doi: 10.1021/acscatal.2c00671.

[15] J. Zhu *et al.*, «Ni–In Synergy in CO_2 Hydrogenation to Methanol», *ACS Catal.*, vol. 11, n.º 18, pp. 11371–11384, set. 2021, doi: 10.1021/acscatal.1c03170.

[16] T. Ukawa, K. Nishide, e Y. Inada, «XAFS Analysis on Reduction Process of Cerium Oxide», 2018.

[17] J. B. Branco, A. C. Ferreira, F. Vieira, e J. F. Martinho, «Cerium-Based Bimetallic Oxides as Catalysts for the Methanation of CO_2: Influence of the Preparation Method», *Energy Fuels*, vol. 35, n.º 8, pp. 6725–6737, abr. 2021, doi: 10.1021/acs.energyfuels.1c00030.